RESISTIVITY SURVEY IN THE HENGILL AREA, SW-ICELAND

Nyambayar Tsend-Ayush
Department of Seismology
Research Center of Astronomy and Geophysics
Mongolian Academy of Science
P.O.Box 152, Ulaanbaatar–51
MONGOLIA
nyambayar@rcag.url.mn

ABSTRACT

Geophysical methods are powerful tools for characterizing geothermal structures at depth. One of these is the TEM method that is an important electrical method in outlining geothermal resources. TEM soundings have proven to be more downward focussed than the traditional DC-soundings and have a better resolution at depth. The resistivity structure of high-temperature geothermal systems is generally characterized by a low-resistivity cap underlain by a high-resistivity core.

Here the results of a detailed TEM resistivity survey in the south-western part of the Hengill volcanic system are described. This survey was an addition to an extensive geophysical survey of the Hengill geothermal area with resistivity soundings added in the southwest part of the area. The TEMTD interpretation program was used to perform 1D inversion on the TEM data. A new iso-resistivity map of the Hengill geothermal system is presented. The results revealed an extension of the geothermal field to the southwest along the fissure swarm connected to the Hengill volcanic system. The high-resistivity core extends along the fissure swarm and reaches an elevation of approximately 100 m b.s.l. This resistivity survey supports the existence of a substantial high-temperature geothermal reservoir in the southwest part of the Hengill central volcano.

1. INTRODUCTION

Geophysics has proven to be a powerful tool in geothermal exploration for decades. In geophysical exploration, the physical properties of the earth's crust are examined. In geothermal exploration the task is the detection and delineation of geothermal resources; the location of exploitable reservoirs and the siting of drillholes, through which hot fluids at depth can be extracted. Most geophysical methods have been applied in geothermal prospecting. In geothermal exploration the most important methods are various electrical and thermal methods. Rocks containing geothermal fluids are usually characterized by anomalously low resistivity. Therefore, those methods which measure the electrical resistivity at depth have been the most useful of all geophysical methods used to prospect for geothermal reservoirs.

Resistivity methods have been used for decades in geothermal surveying in Iceland. From the mid-sixties, DC methods, mostly Schlumberger soundings, were used to identify and delineate high-temperature systems. In the late eighties the DC methods were succeeded by central-loop TEM soundings (Transient Electro-Magnetic). TEM soundings have proven to be more downward focussed and to have a better resolution at depth than the DC methods (Árnason et al., 2000).

A TEM resistivity survey was carried out in the southwest part of the Hengill geothermal field in July 2006. Participation in the survey and the data interpretation of the TEM soundings presented in this report served as the main project of the author during his six months training in the Geothermal Training Programme of the United Nations University (UNU-GTP). The resistivity survey was organized and carried out by the geophysical department of ÍSOR (Iceland GeoSurvey), and the main purpose of this resistivity survey was to define the detailed resistivity structure along the fissure swarm to detect, if possible, an extension of the high-temperature reservoir to the southwest.

A 1D inversion method and 1D horizontal layered model TEMTD program was used for the resistivity data interpretation. TEMTD can be used to invert TEM or MT data and also for joint inversion of TEM and MT data. In this project 1D modelling using TEMTD occam inversion was applied to the data. The results are presented as new iso-resistivity maps at different elevations as well as cross-sections through the southwest part of the Hengill geothermal system.

2. GEOPHYSICAL EXPLORATION

2.1 Introduction

The fundamental parameters of interest which characterize a geothermal system are:

- Temperature;
- Pressure;
- Porosity (water/steam content);
- Permeability; and
- Chemical composition of the fluid.

A good geothermal reservoir has high temperature, high pressure, high porosity and permeability, and a low content of dissolved solids and gases in the water. Most exploration methods estimate the fundamental parameters indirectly (Hersir and Björnsson, 1991). In high-temperature fields, thermal alteration of the rock is the dominant parameter in the resistivity structure of the geothermal system (Árnason et al., 2000).

The most important methods in geothermal exploration are:

- *Geological mapping:* Regional and local stratigraphy, geological formations, volcanism, faults, fissures, dip, thermal springs;
- *Chemical study of thermal water and steam:* Dissolved solids, thermometers, isotopes;
- *Geophysical measurements:* Direct methods (temperature, resistivity), structural methods (seismic, gravity, magnetic); and
- *Exploratory drilling, logging.*

It is not possible to tell from geophysical data alone as to whether or not there is an economically exploitable geothermal system in a certain area. It is essential to combine geophysics with geology, geochemistry and borehole data in order to obtain significant information on the geothermal field under investigation (Hersir and Björnsson, 1991).

The primary aim of geophysical exploration of geothermal areas is to:

- Find geothermal prospects;
- Outline drilling fields;
- Locate aquifers and site wells; and
- Estimate properties of the system.

Geophysical exploration of geothermal areas can be divided into: Surface geophysics (exploration) and borehole geophysics (logging). The success of a geophysical survey is measured by the time, effort and money which the survey has saved in delineating a prospect area and in siting successful wells. The success of a survey is highest if it can be used to lower the total number of drill holes and assist in avoiding the drilling of unsuccessful wells.

Basic geophysical methods measure some physical properties related to the geothermal system. The physical properties must differ from those of the host rock in order to create an anomaly. If the variation in physical properties is related directly to the geothermal system (e.g. temperature), it is studied using direct exploration methods. If the anomaly is caused by associated geological formations or structures, (e.g. dykes, faults), indirect exploration methods are used.

The most important physical properties measured in geothermal exploration are:
- Temperature (°C);
- Electrical resistivity (Ωm);
- Magnetization (A/m);
- Susceptibility (dimensionless) ;
- Density (g/cm^3);
- Elasticity (N/m^2);
- Seismic velocity (m/s);
- Thermal conductivity (W/m°C);
- Electrochemical or streaming potential, SP (V); and
- Radioactivity (in logging).

The best results are often obtained through the combined use of two or more methods.

2.2 Performing a geophysical survey

The first step is to collect all available data on the geothermal field (Hersir and Björnsson, 1991):

- Topographical information; maps 1:50,000 - 1:100,000, accessibility, roads;
- Geological information; maps, geological units, tectonics, fumaroles, alteration ;
- Existing geophysical data; review all available data;
- Drilled wells; geological sections and logs; and
- Geochemistry; minerals in water and steam, chemical thermometers.

The most promising geophysical method is selected by using all available data. A trial survey ought to be carried out, at the least, before a large-scale geophysical campaign is started in a new or unknown area. It is important to stake the area in detail before field measurements start. The best routine depends on the method used. It is important to organize the field setup to minimize time and organize the collected data.

Preparation and presentation of the data: The readings of the field data are converted to appropriate units, corrected if necessary, and then plotted on a map. Two methods are common in presenting geophysical data:

- Iso-anomaly curves or contour lines: Iso-anomaly maps give an overview of the data but usually, not all the details;
- Profiles or sections: The observation station is the abscissa along a line and the measured value (anomaly) is the ordinate on ordinary graph paper. Profiles visualize the continuous variation of anomalies better than contour maps.

Iso-anomaly maps and profiles are summaries of the observations and are not geological interpretations. Some qualitative conclusions can be drawn from these such as: location of an anomalous body, size and form of an anomaly, strike of faults or dykes, etc. A short wavelength anomaly usually reflects shallow depth; a broad anomaly may reflect greater depth. With experience and by considering other data, it is possible to extract good qualitative information from maps and profiles. Quantitative interpretations usually involve a certain amount of computational work depending on the method and, of course, close cooperation with geologists, geochemists and engineers in order to construct a model of the explored field (Hersir and Björnsson, 1991).

2.3 The most important geophysical methods in geothermics

The most important properties of a geothermal system are temperature, permeability and the chemical composition of the fluid. Various parameters are measured in geophysical exploration. An attempt is made to connect them to the properties of the geothermal system. Geophysical methods are divided into direct and indirect or structural methods. The most important geophysical exploration methods in volcanic areas are (Hersir and Björnsson, 1991):

Thermal methods: The most direct method is to study the subsurface temperature in a geothermal system. Temperature is measured in shallow drill holes and in soil. Estimation of the temperature at depth is made from the temperature gradient. Conduction versus convection in geothermal systems is determined, as well as the location of aquifers in geothermal wells.

Electrical resistivity of rocks: The electrical resistivity of rocks is an important parameter which can be related to the properties of geothermal systems. In most rocks near the earth's surface the electrical conduction is mainly electrolytic in an aqueous solution of common salts distributed through the pores of the rock and/or along the rock-water interface. The resistivity depends on the pore structure, amount of water (saturation), and salinity of the water, steam content in the water, water-rock interaction (alteration minerals), temperature and pressure. The salinity of the water, temperature, porosity and water-rock interaction are of greatest influence. Resistivity measurements are used to delineate geothermal systems, locate aquifers and sometimes to estimate porosity and physical conditions within a geothermal system.

DC-resistivity methods: Several types of the direct current resistivity method have been used for decades in geothermal exploration with great success. The most widely used is the Schlumberger method. DC-methods are used both for depth-soundings and profiling. Nowadays, 2D modelling is a standard procedure. Near-surface vertical structures can be delineated. The limitations of the DC-methods include a relatively slow progress in the field, tedious two-dimensional model calculations and limited depth penetration.

AC-resistivity methods: MT, AMT, EM, TEM. The magneto-telluric method has been used for deep probing, mainly in sedimentary basins. Various types of electromagnetic methods and time-domain electromagnetic methods have been used in geothermal exploration. In the last two decades the TEM method with two concentric loops has proven very successful in Iceland. TEM soundings have proven to be more downward focussed and to have better resolution at depth than DC methods (Árnason et al., 2000).

SP survey: This is a low-cost surveying technique and has been applied in many geothermal areas. However, the anomalies are usually small and can be contaminated by noise.

Magnetic survey: A structural method. Numerous aeromagnetic surveys have been carried out over geothermal areas. A correlation between magnetic lows and zones of intense hydrothermal alteration has been found. Detailed ground-magnetic surveys are used in Iceland to trace narrow near surface linear features like dykes and faults where the basement is covered with soil.

Gravity survey: A structural method. This is typically used to find features such as faults, dense intrusions or sediments on a dense basement. It is also used to monitor the fluid mass extraction from a geothermal reservoir by repeated surveying over the reservoir.

Seismicity, micro-earthquakes: Many geothermal systems exist in volcanic tectonically-active areas and are characterized by a high level of micro-seismic activity. Earthquakes can give important information on active fissures through the geothermal system that can imply good permeability within the reservoir and hence heat mining as well as cooling zones. There is, in most cases, no clear one-to-one relationship between the location of micro-earthquakes, and the geothermal reservoir. In some areas micro-earthquakes indicate cooling intrusions.

Seismic methods - Reflection and refraction: Seismic reflection and seismic refraction have both been used, to a limited extent, in geothermal exploration.

Logging in geothermal wells: Logs are performed to give information on well performance, and also to obtain information on lithological structures and physical properties of the geothermal system penetrated by a well.

3. ELECTRICAL RESISTIVITY OF WATER-BEARING ROCKS

Measuring the electrical resistivity of the subsurface is the most powerful prospecting method in geothermal exploration. Resistivity is directly related to the properties of interest, like salinity, temperature, alteration and porosity (permeability). To a great extent, these parameters characterize the reservoir. The electrical resistivity of a material is defined as the electrical resistance in ohms between the opposite faces of a unit cube of the material. For a conducting cylinder of resistance δR, length δL, and a cross-sectional area δA (Figure 1), the resistivity ρ is given by the equation (Hersir and Björnsson, 1991):

FIGURE 1: Parameters used to define resistivity (mod. from Keary and Brooks, 1992)

$$\rho = \frac{\delta R \, \delta A}{\delta L}$$ (1)

where ρ = Resistivity (Ωm);
        δR = Resistance (Ω);
        δA = Area (m^2); and
        δL = Length (m).

The reciprocal of resistivity is conductivity:
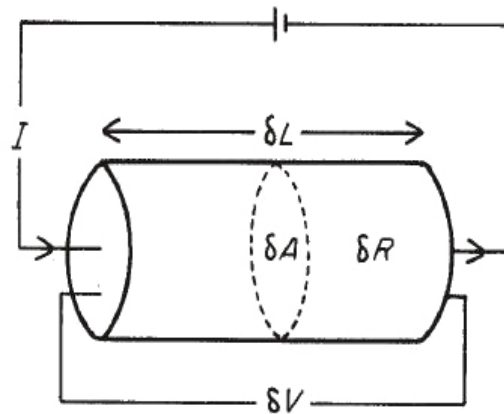
$$\sigma = \frac{1}{\rho} \qquad (2)$$

where σ = Conductivity (S/m).

Equation 1 is used to determine the resistivity of a homogeneous material with a regular geometric shape like a cylinder or cube. The resistivity of a material is defined mathematically according to Ohm's law that states that the electric field strength at a point in a material is proportional to the current density passing through that point (Keller and Frischknecht, 1966).

$$\vec{E} = \rho\vec{j} \quad \text{or} \quad \rho = \left|\vec{j}\right| / \left|\vec{E}\right| \qquad (4)$$

where $\vec{E}$ = Electric field (V/m);
$\vec{j}$ = Current density (A/m^2).

In all resistivity measurements, the surveying is conducted by measuring a signal from a naturally occurring or artificially induced current in the ground. In conventional DC soundings such as Schlumberger soundings, this is done by injecting current through electrodes at the surface and the measured signal is the electric field (potential difference over a short distance) generated at the surface. In magnetotelluric (MT) soundings, the current in the ground is induced by time variations in the earth's magnetic field, and the measured signal is the electric field at the surface as in the DC soundings (Árnason, 1989).

In most rocks near the earth's surface, the conduction is dominated by electrolytic conduction in aqueous solution of common salts distributed through the pores of the rock and/or at the rock-water interface. The rock matrix itself is an insulator. The electrical resistivity of rocks depends on:

- Porosity and permeability of the rock;
- Amount of water (saturation);
- Salinity of the water;
- Temperature;
- Pressure;
- Water-rock interaction and alteration; and
- Steam content in the water.

The most important factors are the porosity, temperature, salinity and the water-rock interaction. In geothermal areas, the rocks are water-saturated. Ionic conduction in the saturating fluid depends on the number and mobility of ions and the connectivity of flowpaths through the rock matrix. The pressure dependence is negligible compared to the temperature dependence, provided that the pressure is sufficiently high so that there is no change in phase (Hersir and Björnsson, 1991).

3.1 Porosity and permeability of the rock

Porosity is defined as the ratio between the pore volume and the total volume of a material. There are primarily three types of porosity.

Intergranular: The pores are formed as spaces between grains or particles in a compact material (sediments, volcanic ash);

Joints-fissures: A net of fine fractures caused by tension and cooling of the rock (igneous rocks, lava);

Vugular: Big and irregular pores, formed as material is dissolved and washed away, or pores formed by gas (volcanic rocks, limestone).

Fluid is important for electrical conduction of a rock, therefore the degree of saturation (dictated by porosity) is of importance to the bulk resistivity of the rock. According to Archie's law (Archie, 1942), resistivity of water-saturated rock varies approximately as the inverse square of the porosity. This law describes how resistivity depends on porosity if ionic conduction dominates other conduction mechanisms in a rock (Hersir and Björnsson, 1991). If the resistivity of the pore fluid is ≤ 2 Ωm, then:

$$\rho = \rho_w a \varphi_t^{-n} \tag{4}$$

where ρ_w = Resistivity of the pore fluid (Ωm);
φ_t = Porosity in proportion to the total volume;
a = Empirical parameter depending on type of porosity that varies from less than 1 for inter-granular porosity and over 1 for joint porosity, usually around 1; and
n = Cementation factor, usually around 2.

According to Archie's law the ratio ρ/ρ_w is constant for a given porosity. This constant is called the formation factor.

$$F = a\phi_t^{-n} = \frac{\rho}{\rho_w} \tag{5}$$

where F = Formation factor.

Permeability of a rock is the ability of fluids to be transmitted within its matrix. Permeability depends on the interconnectivity of the pore spaces within the rock matrix rather than the porosity of the rock. The amount of fluid flowing through a rock can also be largely dictated by fractures (secondary porosity), common in geothermal areas. The wider the fracture, the higher fracture porosity, hence, high permeability as expressed by the following equation (ISL, Michigan State University, 1999):

$$K = \frac{Q\eta L}{AP} \tag{6}$$

where K = Permeability (m^2);
Q = Fluid flowrate (m^3/s);
η = Fluid viscosity (kg/ms);
L = Length of the rock (m);
A = Cross-sectional area available for flow (m^2); and
P = Pressure drop (Pa).

Due to the negligible electrical conduction in most minerals, the majority of charge transport in rocks and sediments occurs in the electrolytes along the water-rock interface. High mobility (due to high permeability) of the charge carrier within a rock matrix has the effect of lowering electrical resistivity of the rock.

Geological processes such as faulting, shearing, columnar jointing and weathering usually increase permeability and porosity, therefore increase electrical conductivity, whereas precipitation of calcium carbonate or silica reduces porosity and hence increases resistivity.

3.2 Resistivity as a function of salinity

An increase in the amount of dissolved ions in the pore fluid increases the conductivity (Figure 2). Conductivity of solutions is a function of salinity and the mobility of the ions present in the solution. This is expressed in Equation 7 (Hersir and Björnsson, 1991):

$$\sigma = \frac{1}{\rho} = F(c_1 q_1 m_1 + c_2 q_2 m_2 + ...) \qquad (7)$$

where
σ = Conductivity (S/m);
F = Faraday's number $(9.65 \times 10^4$ C);
c_i = Concentration of ions;
q_i = Valence of ions; and
m_i = Mobility of ions.

FIGURE 2: Pore fluid conductivity vs. salinity (concentration) for a variety of electrolytes (mod. from Keller and Frischknecht, 1966)

3.3 Resistivity as a function of temperature

The relationship between resistivity and water temperature is shown in Figure 3. At lower temperatures, a rise in the temperature of an electrolytic solution decreases viscosity leading to an increase in ion mobility and lower resistivity (see Equation 7). At high temperatures, a decrease in the dielectric permittivity of water results in a decrease in the number of dissociated ions in a solution. Above 300°C, this starts to increase the fluid resistivity (Quist and Marshall, 1968). At temperatures below 200°C the relationship between the resistivity, ρ, and temperature, T, of the rock saturated with an electrolyte has been approximated by Dakhnov (1962) as:

$$\rho_w = \frac{\rho_{w0}}{1 + \alpha(T - T_0)} \qquad (8)$$

FIGURE 3: Resistivity of an electrolyte as a function of temperature at different pressures (mod. from Ouist and Marshall. 1968)

where
ρ_{w0} = Resistivity of the fluid at temperature T_0;
α = Temperature coefficient of resistivity, $\alpha \approx 0.023$ °C^{-1} for $T_0 = 23$°C and 0.025°C^{-1} for $T_0 = 0$°C.

3.4 Pressure

Confining pressure has the net effect of increasing the bulk resistivity of a rock by decreasing pore volume as the rock is compressed. The pressure effect can be dramatic in fractured rock where the fractures normal to the principle stress close while others remain open. This brings about a significant change and anisotropy of the rock (Morris and Becker, 2001).
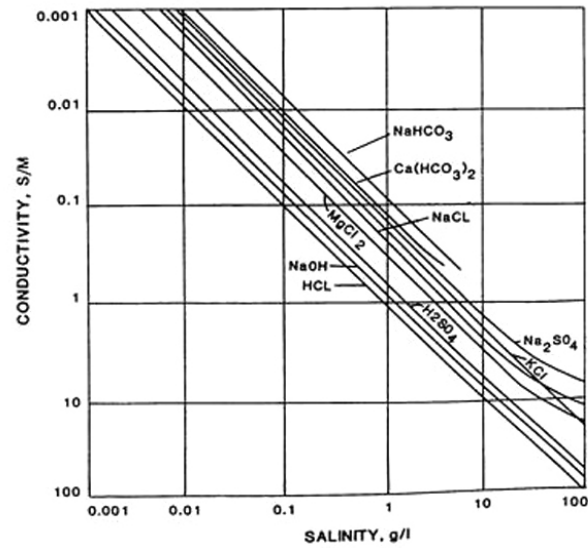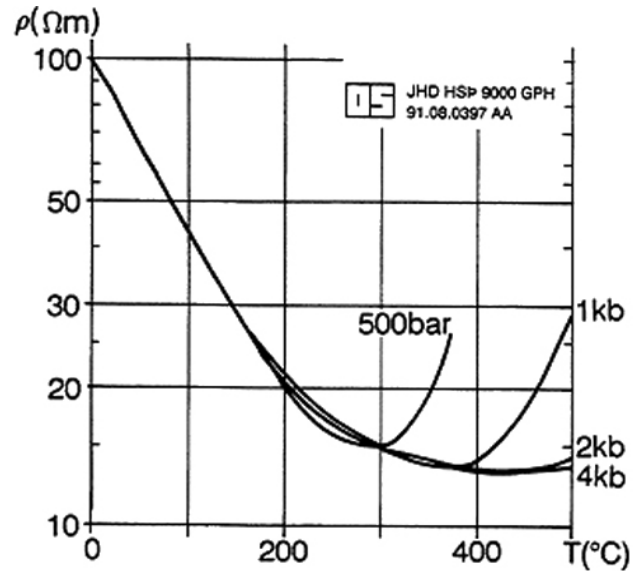
3.5 Resistivity and fluid-rock interaction

Experiments show that Archie's law is only valid for conductive solutions ($\rho_w < 2$ Ωm) (Flóvenz et al., 1985). The bulk resistivity is decreased by surface conduction along the interface between rock and water and conductive alteration minerals. This can be expressed in a formula (Rink and Schopper, 1976):

$$\sigma = \frac{1}{F}\sigma_w + \sigma_s \tag{9}$$

where σ = Bulk conductivity (S/m);
        σ_w = Conductivity of water (S/m);
        F = Formation factor of the rock;
        σ_s = Interface conductivity (S/m).

The interface conductivity σ_s is caused by fluid-matrix interaction. Experiments show that interface conductivity depends more on the magnitude of the internal surface (porosity) and on their nature (surface conditions) than on the original chemical composition of water and rock. The two main reasons for interface conductivity are the presence of clay minerals (alteration) and the surface double-layer conduction (Hersir and Björnsson, 1991).

3.6 Resistivity structure of high-temperature geothermal systems

The resistivity structure of high-temperature geothermal systems is generally characterized by a low-resistivity cap at the outer margins of the reservoir, underlain by a more resistive core towards the inner part. This structure has been found in both freshwater systems as well as brine systems, with the latter having lower resistivity values. Comparison of this resistivity structure with data from wells has been carried out in high-temperature geothermal fields, in Iceland (Árnason et al., 2000) (Figure 4).

Resistivity is relatively high in cold unaltered rocks outside the reservoir and moderate at temperatures of 50-100°C, as alteration intensity is

FIGURE 4: The resistivity structure summarised
(mod. from Árnason et al., 2000)

normally low in this temperature range. At temperatures of 100-230°C, low-temperature zeolites and smectite are formed, with high conductivity and low resistivity. In the temperature range of about 230-250°C, resistivity increases again towards the interior of the reservoir, within the mixed layer clay zone. At about 250°C, the smectite disappears and chlorite becomes the dominant mineral. At even higher temperatures, about 260-300°C, epidote becomes abundant in the so-called chlorite-epidote zone. The minerals chlorite and epidote are highly resistive, since the chlorite minerals have cations that are fixed in a crystal lattice, making the mineral resistive. The chloride-epidote zone, therefore, corresponds to the resistive core (Árnason et. al., 2000).
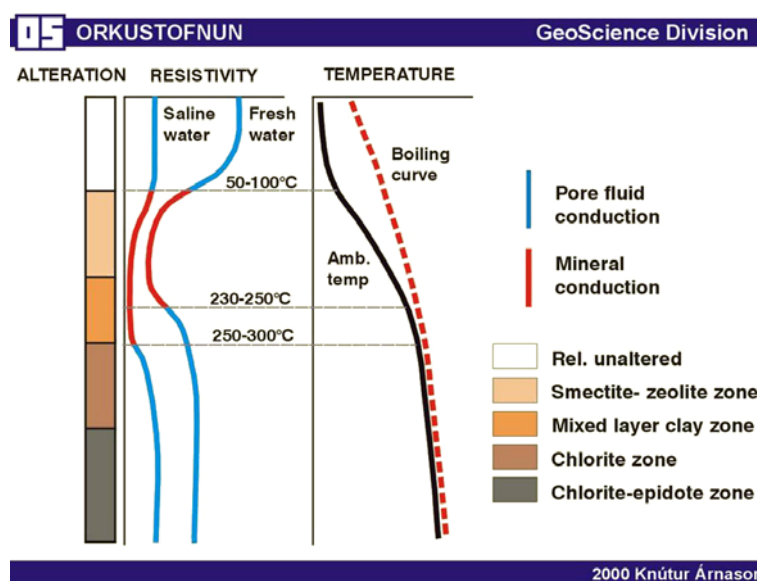
4. ELECTROMAGNETIC RESISTIVITY METHODS

4.1 Introduction

Electromagnetic resistivity methods make use of an alternating current (AC-current) induced in the earth. The alternating current may be artificially induced, as in TEM, or be natural signals, as in MT. Until in the eighties, these methods were not widely used in geothermal exploration. The two main categories of electromagnetic methods depend on the different sources of the alternating current. They are:

- Natural-source electromagnetics – MT and AMT;
- Controlled-source electromagnetics - TEM (central-loop). In this report, the focus is on the TEM sounding method.

4.2 The central-loop Transient Electromagnetic method (TEM)

In the central-loop TEM sounding method, the current in the ground is induced by a time - varying magnetic field of a controlled magnitude generated by a source loop. A loop of wire is placed on the ground and a constant magnetic field of known strength is built up by transmitting a constant current into the loop. The current is then abruptly turned off. The decaying magnetic field induces electrical currents in the ground (see Figure 5). The current distribution in the ground generates a secondary magnetic field decaying with time. The decay rate of the secondary magnetic field is monitored by measuring the voltage induced in a receiver coil at the centre of the transmitting loop. The current distribution and the decay rate of the secondary magnetic field depend on the resistivity structure of the earth. The decay rate, recorded as a function of time after the current in the transmitter loop is turned off, can, therefore, be interpreted in terms of the subsurface resistivity structure (Hersir and Björnsson, 1991).

The induced voltage in a receiver coil at the centre of a circular source loop at radius *r* with harmonic current, $I = I_0 e^{iwt}$ on the surface of a layered half-space (Figure 6) is given as (Árnason, 1989):
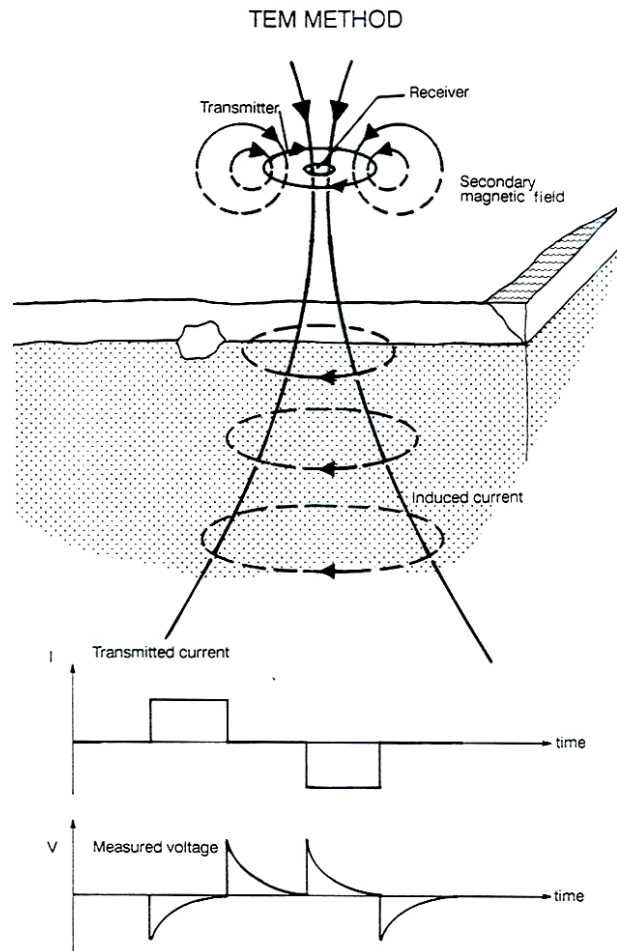
FIGURE 5: The central loop TEM sounding configuration (mod. from Hersir and Björnsson, 1991)

$$V(\omega, r) = A_r n_r A_s n_s I_0 e^{i\omega t} \frac{-i\omega\mu_0}{\pi r} \int_0^\infty \frac{\lambda^2}{m_0} \frac{S_0}{S_0 - T_0} J_1(\lambda r) d\lambda \qquad (10)$$

where A_r = Cross-sectional area of the receiver coil (m²);
      n_r = Number of windings in the receiver coil;
      μ_0 = Magnetic permeability in vacuum (H/m);

$\quad A \qquad$ = Cross-sectional area of the transmitter loop (m^2)
$\quad n_s \qquad$ = Number of windings in the transmitter loop;
$\quad r \qquad$ = Radius of transmitter loop (m).

S_0 and T_0 are given by the recursion relations:

$$S_{i-1} = S_i \cosh(m_i d_i) - T_i \sinh(m_i d_i)$$

$$T_{i-1} = \frac{m_i}{m_{i-1}} \left[S_i \sinh(m_i d_i) - T_i \cosh(m_i d_i) \right]$$

$$S_{N-1} = 1 ; \qquad T_{N-1} = \frac{m_N}{m_{N-1}}$$

where $\quad d_i \qquad$ = Thickness of the i'th
$\qquad\qquad\qquad$ layer (m); and
$\qquad m_i \qquad$ = Impedance of the i'th
$\qquad\qquad\qquad$ layer.

The quantities S_0 and T_0 which determine the voltage in Equation 10 depend on ω and the conductivities, σ_i through

FIGURE 6: The N layered eart
(mod. from Árnason, 1989)

$m_i = \sqrt{\lambda^2 - k_i^2}$ where $k_i^2 = \omega^2 \mu_i \varepsilon_i - i\omega\mu_i \sigma_i$ (ε is the dielectric permittivity); $i = 0, 1, \ldots N$. In the quasi-stationary approximation $\varepsilon \sim 0$, $k^2 = i\omega\mu\sigma$.

Mutual impedance between the source and the receiver coil (by analogy with Ohm's law) is defined by the ratio between the measured voltage and the transmitted current. From Equation 10, the mutual impedance is:

$$Z(\omega, r) = \frac{V_L(\omega, r)}{I_0 e^{i\omega t}} = A_r n_r A_s n_s \frac{-i\omega\mu_0}{\pi r} \int_0^\infty \frac{\lambda^2}{m_0} \frac{S_0}{S_0 - T_0} J_1(\lambda r) d\lambda \qquad (11)$$

Equation 11 can be transformed to the time domain by Fourier expansion of the function describing the transmitted current (Árnason, 1989). If the transmitted current is described by the function $I(t)$, a Fourier expansion of the current function will be:

$$I(t) = \frac{1}{(2\pi)^{1/2}} \int_{-\infty}^{\infty} \tilde{I}(\omega) e^{i\omega t} d\omega \qquad (12)$$

where

$$\tilde{I}(\omega) = \frac{1}{(2\pi)^{1/2}} \int_{-\infty}^{\infty} I(t) e^{-i\omega t} dt \qquad (13)$$

From Equation 12, the induced voltage in the receiver coil in terms of mutual impedance (as a function of frequency) and the Fourier transform of the transmitted current are expressed as:

$$V(t, r) = \frac{1}{(2\pi)^{1/2}} \int_{-\infty}^{\infty} Z(\omega, r) \tilde{I}(\omega) e^{i\omega t} d\omega \qquad (14)$$
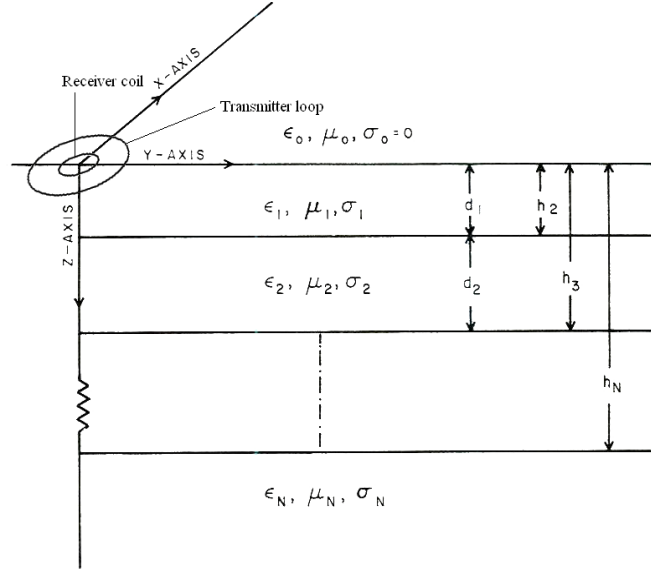
For a constant current *I* turned off at $t = 0$, $\tilde{I}(\omega) = -I/i\omega$. The measured voltage as a function of time after the steady current is abruptly turned off at $t = 0$ is then expressed by:

$$V\_(t) = \frac{-I_0}{2\pi} \int\limits_{-\infty}^{\infty} \frac{Z(\omega)}{i\omega} e^{i\omega t} d\omega = \frac{I_0}{2\pi} \int\limits_{-\infty}^{\infty} \Phi(\omega) e^{i\omega t} d\omega \tag{15}$$

Here for simplicity, we define:

$$\Phi(\omega) = \frac{Z(\omega)}{-i\omega} \tag{16}$$

$\Phi(\omega)$ only depends on ω through ω^2 and $i\omega$, hence:

$$\Phi^*(-\omega) = \Phi(\omega) \tag{17}$$

where * denotes the complex conjugation.

Therefore:

$$\operatorname{Re}\Phi(-\omega) = \operatorname{Re}\Phi(\omega) ; \qquad \operatorname{Im}\Phi(-\omega) = -\operatorname{Im}\Phi(\omega) \tag{18}$$

Equation 15 can then be simplified to:

$$V\_(t) = \frac{2I_0}{\pi} \int\limits_{-\infty}^{\infty} \operatorname{Re}\Phi(\omega)\cos(\omega t)d\omega \quad \text{as} \quad V\_(t) = \frac{-2I_0}{\pi} \int\limits_{-\infty}^{\infty} \operatorname{Im}\Phi(\omega)\sin(\omega t)d\omega \tag{19}$$

In practice the current is not abruptly turned off, but turned off linearly in a time interval of length *TOFF*. Transient voltage generated in the receiver coil due to a linearly ramped step function is given by (Árnason, 1989):

$$V(t) = \frac{I_0}{TOFF} \int\limits_{-TOFF}^{0} V\_(t - \tau)d\tau = \frac{I_0}{TOFF} \int\limits_{t}^{t+TOFF} V\_(-\tau)d\tau \tag{20}$$

For a homogeneous half-space of conductivity σ, the induced voltage in the receiving coil, at late time after current turn-off, is given approximately by (Árnason 1989):

$$V(t,r) \approx I_0 \frac{C(\mu_0 \sigma r^2)^{3/2}}{10\pi^{1/2}t^{5/2}}, \quad \text{where} \quad C = A_r n_r A_s n_s \frac{\mu_0}{2\pi r^3} \tag{21}$$

This can be solved to obtain the resistivity at the half-space. The formula is then used to define the so-called late-time apparent resistivity (Árnason 1989):

$$\rho_a = \frac{\mu_0}{4\pi} \left[\frac{2I_0 A_r n_r A_s n_s}{5t^{5/2}V(t,r)} \right]^{2/3} \tag{22}$$

where t = Time elapsed after the transmitter current is turned to zero (s);
            A_r = Cross-sectional area of the receiver coil (m^2);
            n_r = Number of windings in the receiver coil;
            μ_0 = Magnetic permeability in vacuum (H/m);

A_s = Cross-sectional area of the transmitter loop (m^2);
n_s = Number of windings in the transmitter loop;
I_0 = Transmitter current (A);
$V(t,r)$ = Measured voltage (V).

5. DESCRIPTION OF THE SURVEY

The Hellisheidi geothermal system is located in the southwest part of the Hengill central volcano. The prospect area is the Eldborg field in the southwest extension of the Hengill fissure swarm (Figure 7). The geothermal area within the Hengill volcanic system is referred to as the Hengill geothermal area, but it includes several geothermal production fields; such as the Hellisheidi field and the Nesjavellir field. The purpose of the survey was to see if the geothermal area has an extension to the southwest along the fissure swarm. In an earlier survey, an indication of the existence of a high-resistivity core was found in the southwest part of the Hengill area (Árnason 2006a). The main purpose of this project was to define the detailed resistivity structure of the Eldborg area. This is done by presenting contour maps and cross-sections of the prospect area, based on TEM soundings.
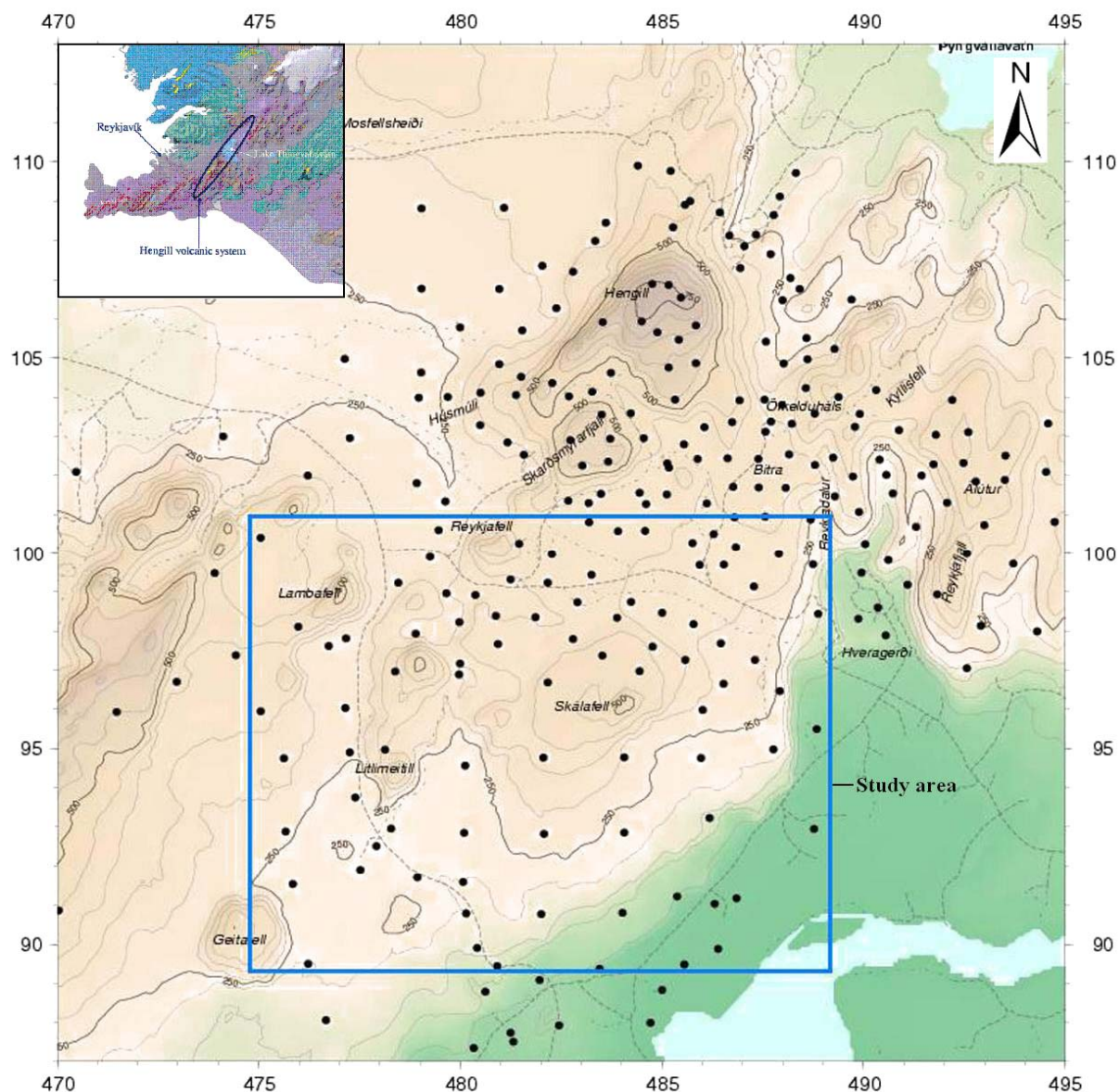
FIGURE 7: The prospect area within the Hengill geothermal system

5.1 Geology of Hengill area

Investigation of the Hengill volcanic complex indicates that super critical conditions are found at a shallow depth, 5 km, and perhaps at less than 3 km depth associated with the youngest volcanic structure in the western part of the Nesjavellir system. The Hengill volcanic system is active, and it is estimated to discharge a power of 1000 MWe. The Hengill volcanic complex is divided into the Hveragerdi-Grensdalur (Graendalur) volcanic system (eastern part of the area) that was active between 700,000 and 30,000 years ago, but is now partially eroded down to the chlorite zone, the Hrómundartindur system, whose surface formations are younger than 115,000 years, and the currently active Hengill system (Fridleifsson et al., 2003).

The Hengill mountain was mostly accumulated in one or two large sub glacial eruptions during the last glacial period. New geological data presented in 2002 suggest that the lower part of the mountain may have formed during the next to last glacial period (Fridleifsson et al., 2003). Hyaloclastite deposition, a typical formation in Iceland, is a fine, glassy debris formed by the sudden contact of hot and coherent magma with either cold water or water-saturated sediments, usually associated with glaciers. The Hengill triple junction in SW-Iceland sits between the Reykjanes Peninsula rift zone, the western volcanic rift zone, and the South Iceland Seismic (transform) zone. Geology of the Hellisheiði geothermal field is characterized by the presence of two kinds of common formations, hyaloclastite formations and basaltic fissure lavas produced in an active fissure swarm.

There are two main volcanic fissures in the Hengill area, of Holocene age, trending NE-SW, that have fed the last volcanic eruptions in the area, extending from Lake Thingvallavatn in the northeast part of the Hengill area (Nesjavellir high-temperature field) extending about 20 km, to the southwest of Hengill mountain (Hellisheidi). The age of the older one is about 5500 years and the younger one is about 2000 years old (Saemundsson, 1967). The lava flows are widespread and cover a large part of the Hellisheidi area. These eruptive fissures and parallel faults control up and out-flow of hot water and steam from the centre of the Hengill system. Tectonic activity is episodic and accompanied by rifting and major faulting along the fissure swarm that intersects the Hengill central volcano, and by magma being injected into the fissure swarm. A row of small craters is marked along both the older and younger eruptive fissures.

5.2 TEM survey and equipment

The field work of the TEM survey was carried out by a field crew of Iceland Geosurvey (ÍSOR), supervised by its specialists in the TEM method. For the TEM resistivity survey, the Time Domain Electro Magnetics Protem digital receiver and a TEM-67 transmitter of Geonics Ltd. was used. A total of 17 new TEM soundings were carried out in the study area and added to existing TEM soundings from previous surveys (Figure 8). In all soundings, a 90,000 m^2 (300 × 300m) transmitter wire loop was used. The receiver loops are a small coil with an effective area of 100 m^2, and a flexible loop with an effective area of 5613 m^2. The maximum transmitted current is usually in the range of 18-20 A, transmitted at the high frequency of 25 Hz, and low frequency of 2.5 Hz. The integration time is 8, 15 and 30 s, and 30 measuring gates time gates are evenly spaced on log-scale from 0.08-8 ms after current turn off. Repeated transients are stacked and stored in the computer memory of the receiver and later downloaded to a PC computer (Geonics Ltd., 1980).

Time Domain Protem systems are now also routinely used for general geological exploration such as for freshwater aquifers in bedrock fractures, and mapping groundwater contaminant plumes. Mapping to the shallow depths required in these applications requires a very wide bandwidth and many narrow sampling gates.
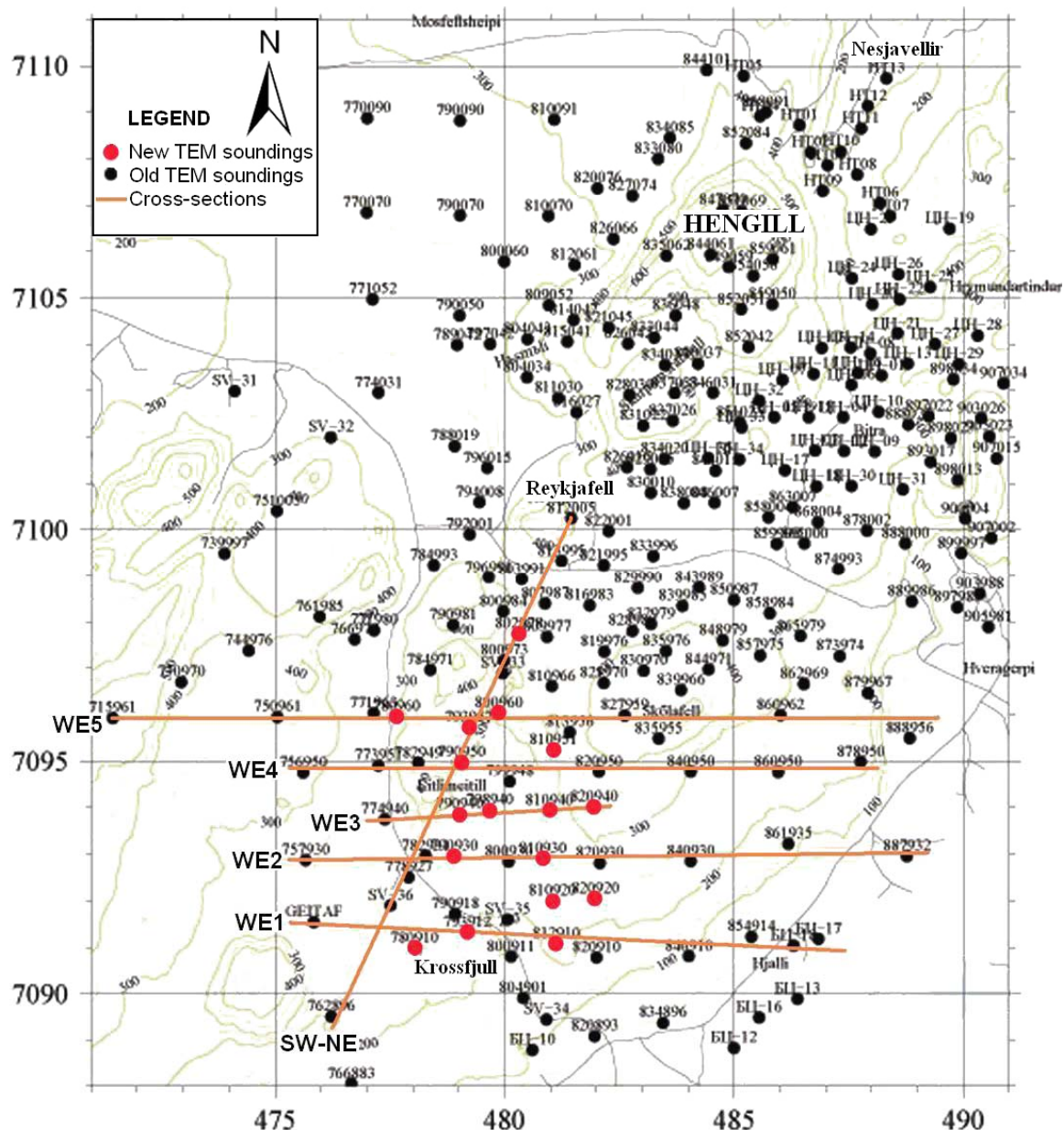
FIGURE 8: Locations of TEM soundings and resistivity cross-sections

5.3 Data processing and interpretation

The recorded raw data were edited using the Multi Edit program of the UNIX/LINUX operating systems, and saved into a TEM sounding data file for each sounding. In the data interpretation process the TEMTD program was used, and the input file containing the measured TEM data was required to have the output format produced by the program TEMX. TEMX reads raw data files from Geonics Protem receivers and calculates averages and standard deviations for repeated transient voltage measurements, as well as late time apparent resistivity as a function of time. The TEMX-program also offers, through a graphical interface (GUI), the possibility of rejecting noisy readings.

The input TEM data file has a header containing different information, such as: the name of the sounding, date of recording, place, coordinates and elevation, size of the source loop, transmitted current, turn-off time and the effective area of the receivers. The header is followed by the measured data segment.

The program TEMTD was developed by Knútur Árnason (2006b), in ANSI-C and runs under UNIX/LINUX operating systems. It uses the Gnuplot graphic program for graphical display during the inversion process. TEMTD reads and stores the header, which is written to the output file. It then reads the recorded data and uses the source loop area to calculate the side length of the loop (assuming it is a square) and uses the current and turn-off time values for calculating model responses. The program TEMTD performs 1D inversion with horizontally-layered earth models of central-loop Transient Electro-Magnetic (TEM) and MagnetoTelluric data. It can be used to invert only TEM or MT data and also for joint inversions of TEM and MT data, in which case it determines the best static shift parameter for the MT data. For TEM data, the program assumes that the source loop is a square and that the receiver coil/loop is at the centre of the source loop. The current wave form is assumed to be a half-duty bipolar semi-square wave (equal current-on and current-off segments), with exponential current turn-on and linear current turn-off. For MT data, the program assumes standard EDI format for the impedance and/or apparent resistivity and phase data.

The forward algorithm for MT is the standard complex impedance 1D recursion algorithm. For TEM, the forward algorithm uses standard recurrence relations to calculate the kernel function for the vertical magnetic field due to an infinitesimal grounded dipole with harmonic current on the surface of horizontally-layered earth (Árnason, 1989; Ward and Hohmann, 1987). The J1 Hankel transform for calculating the frequency domain response of the dipole (Equation 11) is performed by using the J1 digital filter of Anderson (1979). The Fourier transform to the time domain is performed by using the sine-transform of the imaginary part of the frequency domain response (Equation 19) (Árnason, 1989). The sine-transform is performed using the sine digital filter of Anderson (1979).

The inversion algorithm used in the program is the Levenberg-Marquardt non-linear least square inversion as described by Árnason (1989). The misfit function is the root-mean-square difference between measured and calculated values (*chisq*) in Equation 23, weighted by the standard deviation of the measured values. The user can choose whether the program fits the measured voltage values or the late time apparent resistivity values. The program offers the possibility of keeping models smooth, both with respect to resisitivity variations between layers (actually a logarithm of conductivities) and layer thicknesses (actually a logarithm of ratios of depth to the top and bottom of layers). The damping can be done both on "first derivatives", which counteracts sharp steps in the model (on a log scale), and on "second derivatives", which counteract oscillations in the model values (on a log scale). The actual function that is minimised is, in this case, not just the weighted root-mean-square misfit, chisq. The "potential" is:

$$Pot = chisq + \alpha \times DS1 + \beta \times DS2 + \gamma \times DD1 + \delta \times DD2 \qquad (23)$$

where $DS1, DS2$ = The first and second order derivatives of log-conductivities in the layered model;

       $DD1, DD2$ = The first and second order derivatives of the logarithms of the ratios of layer depths;

       $\alpha, \beta, \gamma, \delta$ = The relative contributions of the different damping terms and are specified by the user.

The program can be used to perform minimum structure Occam's inversions. By minimum structure, or Occam's 1D inversion of electromagnetic data, people generally mean that the data are interpreted with many layers with fixed thicknesses and variable resistivities, but the variation of the resistivity values is kept smooth with little contrast between the layers. The initial model can either be automatically generated with constant initial resistivities as described above, or by specifying an initial model file and the resistivities of the layers in the Occam model are adjusted to the resistivity at the corresponding depth in the specified layered model.

Once the input data (measured data, the model and options) have been supplied, the program starts the iterative adjustment of the model. If both TEM and MT data are inverted, the programme also adjusts

the static shift multiplier for the MT apparent resistivity. In each iteration step, the program prints out, to the output device standard error, some information of the progress of the inversion. At the end of the iteration process, the program writes the final model.   Examples of TEM soundings and data interpretation are given in Appendix I which shows all TEM soundings measured for this project. The interpretation of the soundings assumes the number of layers to be between 13 and 20.

The programs TEMRESD, TEMCROSS, TEMMAP were used for all plots of resistivity, the iso map, resistivity cross-section and location of soundings. These programs were developed by Dr. Hjálmar Eysteinsson at ÍSOR, and they all use the GMT system in the environment of UNIX/LINUX operating systems. The program TEMRESD plots out resistivity sections at any depth, using output from Occam's inversion to generate a resistivity iso-map at particular depth.

The program TEMCROSS plots out resistivity cross-sections from results in plot files which are the output files from the layered 1D inversion. The program TEMMAP plots the location of TEM and MT soundings on a map in the UTM coordinate system (or a given coordinate system). It also draws the location of resistivity cross-sections if requested.

6. RESULTS

6.1 General

Resistivity methods are used in geothermal exploration as they reflect the thermal alteration of the rocks dependent on temperature. This observation is of great importance, because the temperature dependence of the alteration mineralogy makes it possible to interpret the resistivity layering in terms of temperature in the reservoir, provided that the temperature is in equilibrium with the dominant alteration minerals.

The purpose of this TEM resistivity survey was to reveal the resistivity structure of the southwest part of the fissure swarm connected to the Hengill central volcano. The aim was to study the resistivity structures of the area in order to define the detailed boundary of the geothermal field and to verify the existence of a high-resistivity core below a low-resistivity cap and, hence, an extension of the geothermal field along the fissure swarm.

The 1D inversion models of the TEM soundings from the TEMTD program were used to create the iso-resistivity maps and cross-sections. The resistivity structure of the study area is presented in six resistivity cross-sections (WE1-WE6) crossing the major fissure swarm, as well as by iso-resistivity maps at different elevations, from sea level down to 850 m below sea level. The location map of the soundings and the resistivity cross-sections is shown in Figure 8.

6.2 TEM resistivity contour maps

The results of a TEM resistivity survey are often presented as iso-resistivity maps showing resistivity at different elevations. Here the results are presented as resistivity maps at sea level and at 500, 600 700 and 850 m b.s.l. (Figures 9-13). All resistivity maps show the results from all soundings in the Hengill area (Árnason, 2006a). The study area is the southwest part of the Hengill area. Within it, the low-resistivity cap reaches up to 200 m a.s.l. in sounding 803991 and the high-resistivity core reaches 100 m b.s.l. in sounding 807987. The following discussion deals only with the study area.

Iso-resistivity map at 0 m a.s.l. Figure 9 shows the resistivity structure at sea level, based on results from the 1D resistivity occam inversion models. It shows clearly that two elongated areas with low resistivity stretch towards the southwest from the Hengill field. One lies clearly along the fissure

swarm which is our area of interest. It shows the top of the low resistivity cap as it stretches towards the southwest.

Iso-resistivity maps in Figures 10-13 show resistivity structures at 500 m b.s.l., 600 b.s.l., 700 b.s.l. and 850 m b.s.l. They show the top of the low-resistivity cap and then the high-resistivity core as the maps cut the core with increasing depth. They show that the high-resistivity core forms a NE-SW trending ridge along the fissure swarm. In the depth range down to 700 m b.s.l. the high-resistivity core is not uniform, but forms separate tops along the ridge.
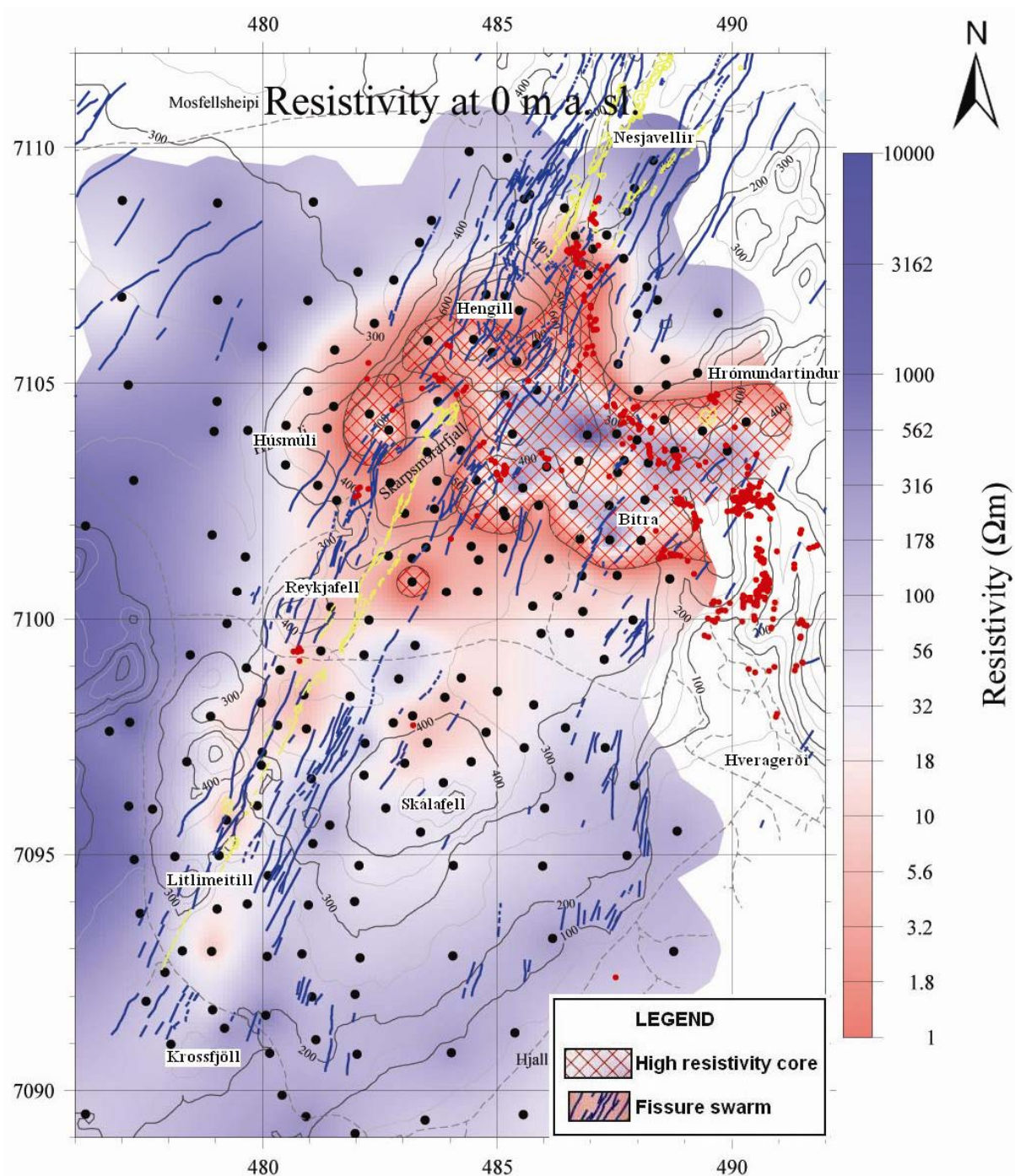
FIGURE 9: TEM resistivity distribution at sea level

The iso-resistivity map at 850 m b.s.l. (Figure 13) cuts clearly through a high-resistivity core in the study area. It shows the characteristics of a high-temperature geothermal field with a high-resistivity core below a low-resistivity cap and it verifies an extension of the Hengill geothermal field to the southwest along the fissure swarm. This map shows clearly that the high-resistivity core forms separate tops along the fissure swarm and the largest and most prominent is the one at the extreme southwest end. It is approximately 4.5 km^2 in size and shows an elongated shape with NW-SE trend or the same trend as seen in the high-resistivity core of the greater Hengill area.
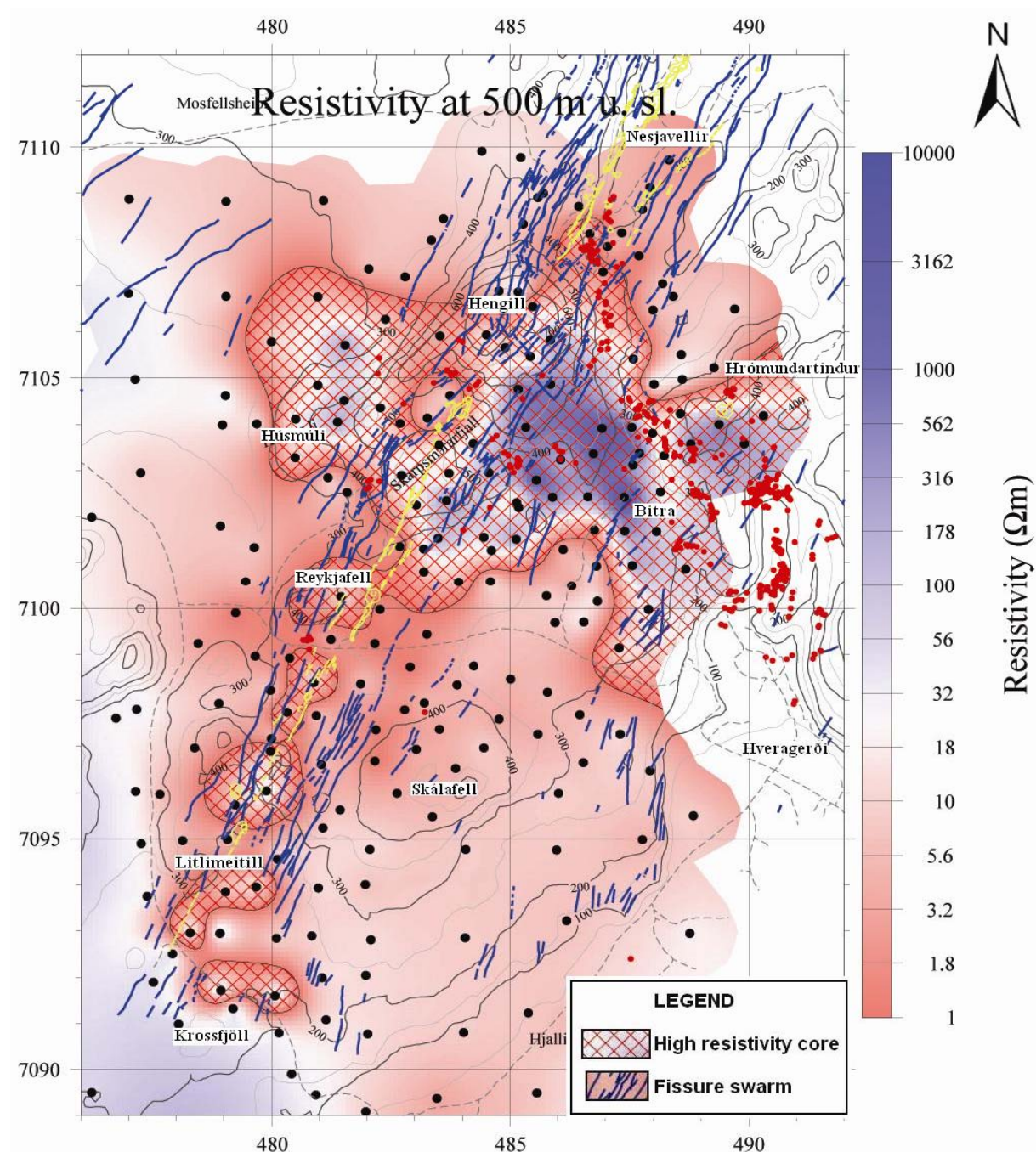
FIGURE 10: TEM resistivity distribution at 500 m b.s.l.
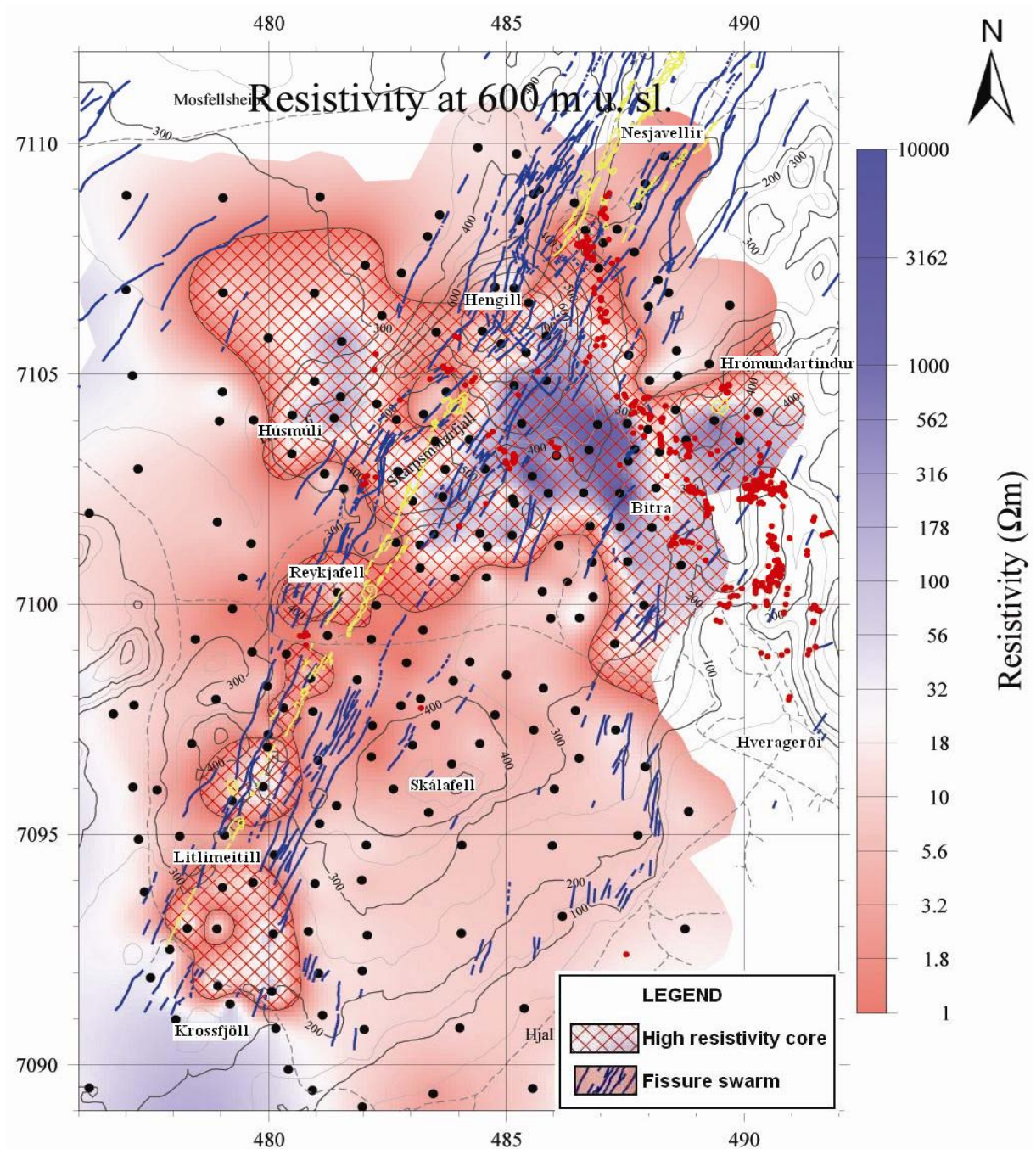
FIGURE 11: TEM resistivity distribution at 600 m b.s.l.
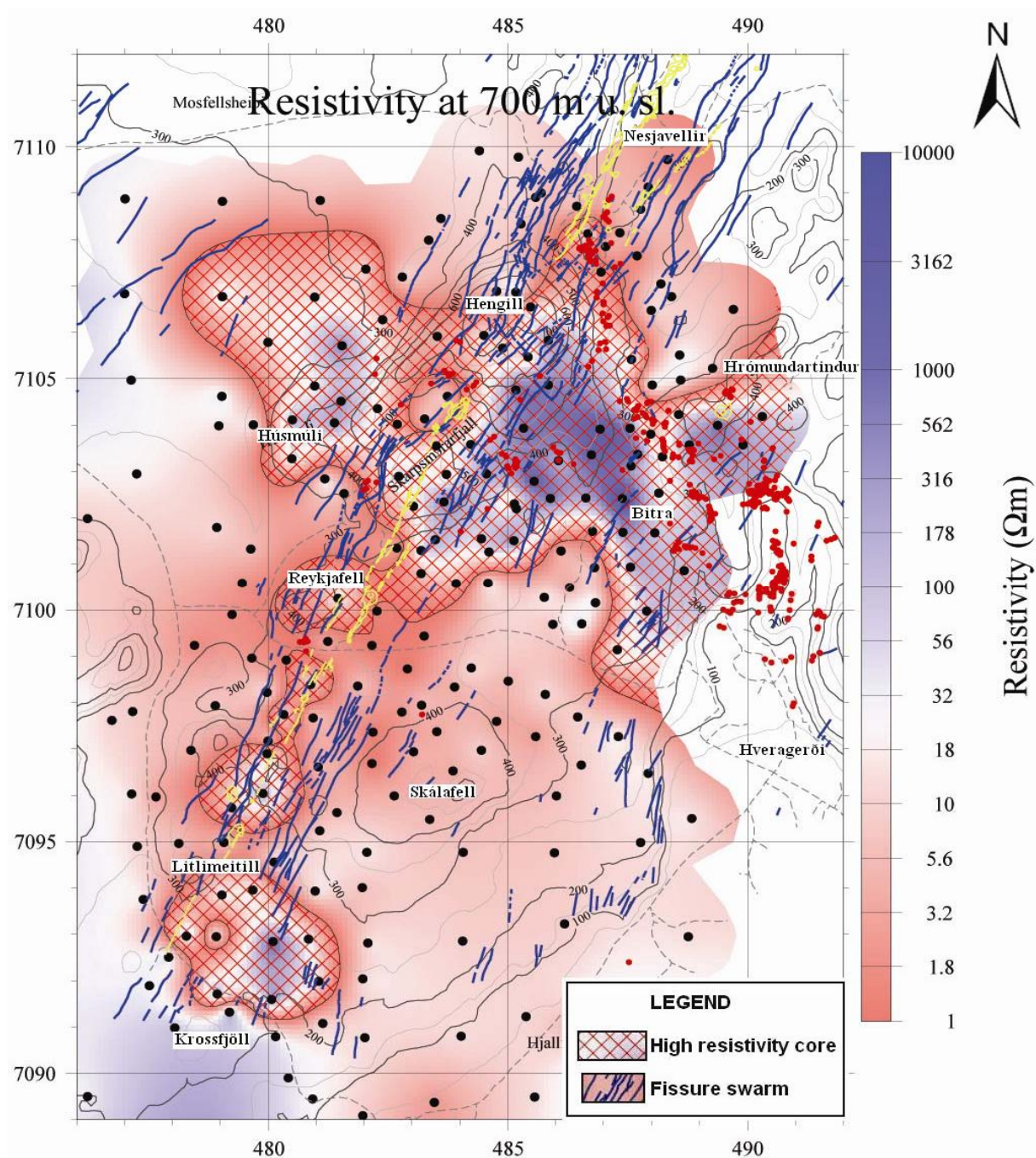
FIGURE 12: TEM resistivity distribution at 700 m b.s.l.
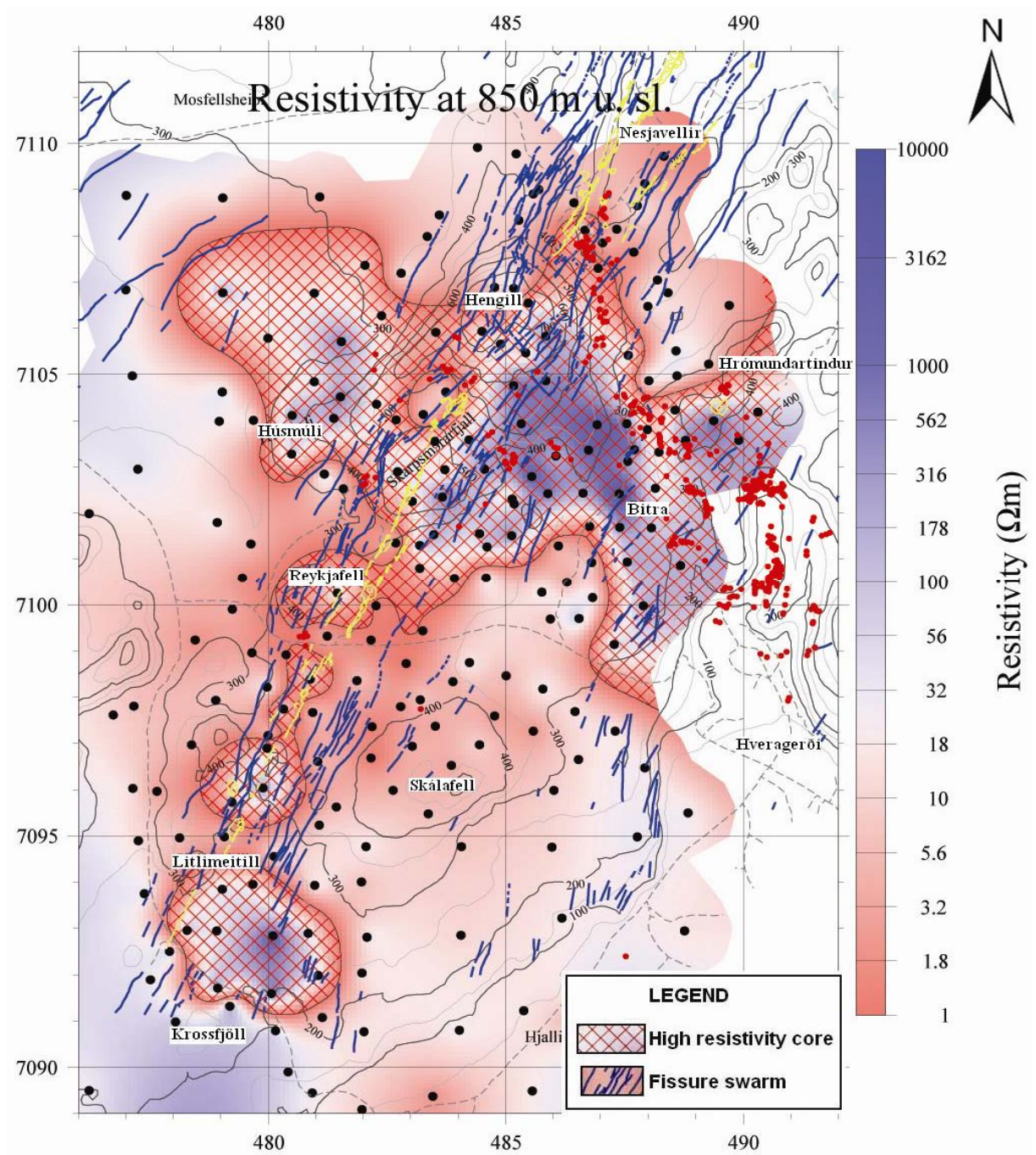
FIGURE 13: TEM resistivity distribution at 850 m b.s.l.

6.3 TEM cross-sections

The characteristics in the resistivity structure of the high-temperature fields in Iceland are a low-resistivity cap underlain by a high-resistivity core. The low-resistivity is defined by resistivity values in the range of 1-10 Ωm in freshwater systems. The high-resistivity core has resistivity values of at least an order of a magnitude higher than that of the low-resistivity cap. The outer margin of the low-resistivity cap delineates the high-temperature field.

The resistivity structure is presented in five resistivity cross-sections from west to east crossing the fissure swarm and in one cross-section from southwest to northeast along the fissure swarm. Their locations are shown on Figure 8.

Resistivity cross-section WE1 (Figure 14) crosses the southernmost part of the study area. The low resistivity cap dips on both sides and thickens to the east. In the easternmost sounding in the cross-section there is an indication of an increase in resistivity under the low-resistivity, but we have no more information on that in other soundings; more soundings are needed to verify that. These soundings are within the Hjalli low-temperature field in the Ölfus area (Georgsson, 1989) and reflect the resistivity structures associated with fossile alteration.
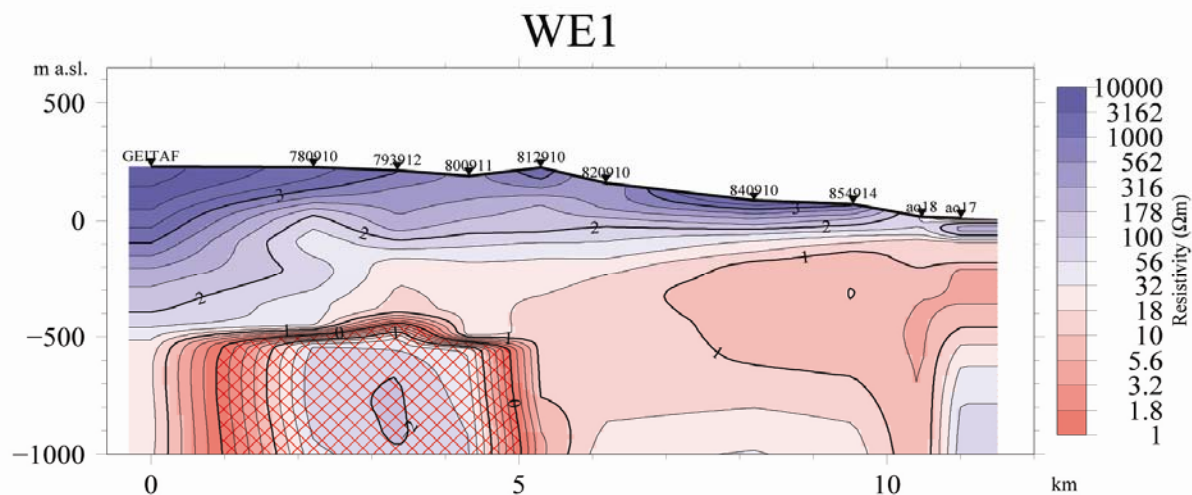

FIGURE 14: TEM resistivity cross-section WE1

Resistivity cross-section WE2 (Figure 15) crosses the study area from west to east. This cross-section shows a low-resistivity cap, and a high-resistivity core and other resistivity structures. In four TEM soundings in the west part of the section (782931, 790930, 800930, 810930) a high-resistivity core below a low-resistivity cap is indicated. The high-resistivity core reaches an elevation of about 300 m b.s.l. at sounding 782931. The 790930 sounding indicates an interesting resistivity structure. In this sounding, a thin low-resistivity layer is seen at about 150 m depth; at about 300 m depth, the resistivity increases again. This high resistivity is considered to reflect unaltered rocks. Furthermore, the low resistivity reaches down to approximately 700 m depth. In this cross-section, the high-resistivity core is approximately 5 km wide. As in cross-section WE1, the low resistivity thickens to the east of the high-resistivity core.

Resistivity cross-section WE3 (Figure 16) crosses the northern part of the main high-resistivity core seen in WE1 and WE2 from west to east. The high-resistivity core is seen at about at 300 m b.s.l. in TEM sounding 798940 and at about 600 m b.s.l. in TEM sounding 790940. The resistive unaltered rock indicated between the two low-resistivity layers in TEM sounding 790940 is discussed above under cross-section WE2.
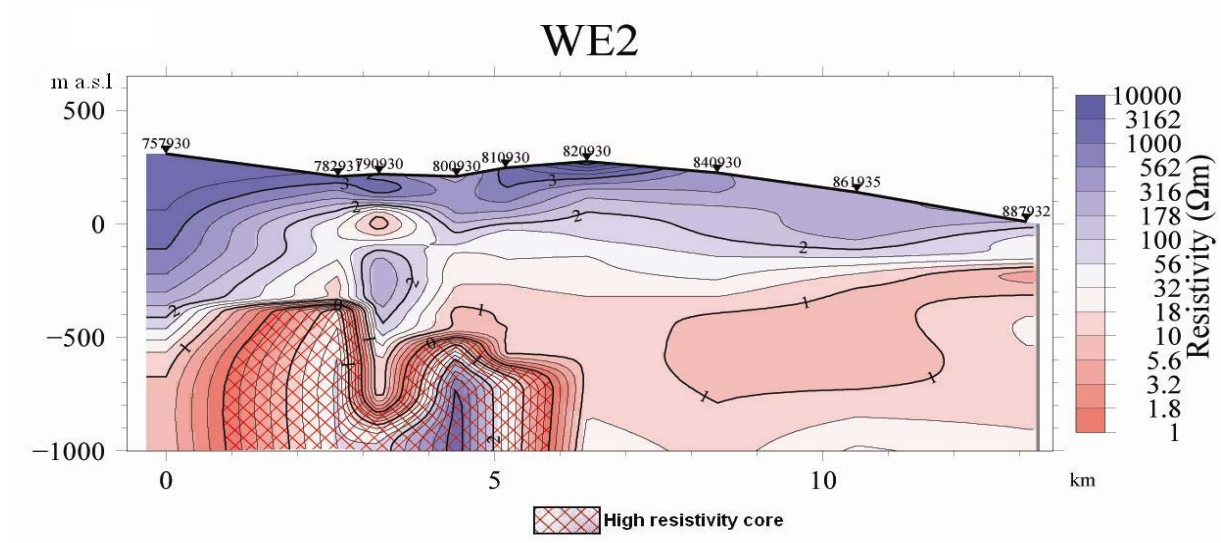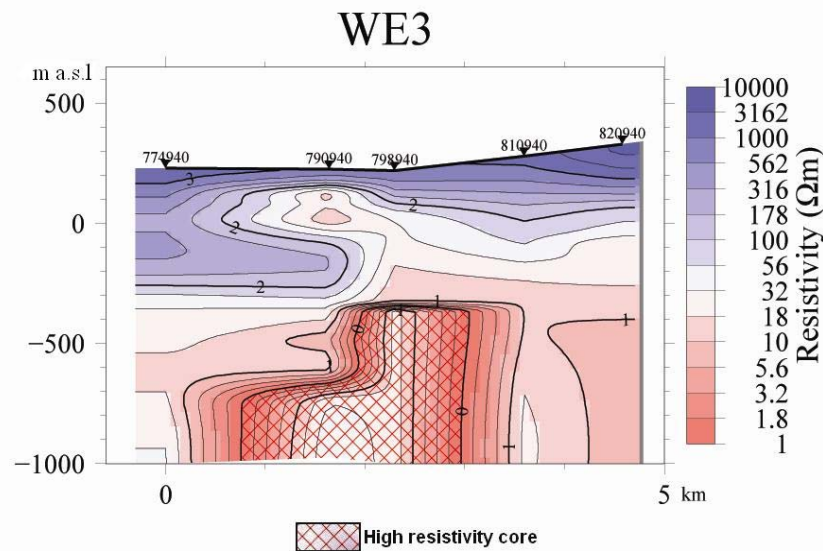
FIGURE 15: TEM resistivity cross-section WE2

FIGURE 16: TEM resistivity cross-section WE3

Resistivity cross-section WE4 (Figure 17) crosses the central part of the study area. This cross-section shows low resistivity layers and other resistivity structures. Most important is the thick low resistivity layer, but there is no sign of a high-resistivity core below. As seen on the resistivity maps and in the SW-NE cross-section (see below), the high resistivity core is not continuous in this depth range (down to 850 b.s.l.) and this cross-section crosses between two tops of the core. The low resistivity layer is thick to the east with a hint of resistivity increase with depth.

Resistivity cross-section WE5 (Figure 18) cuts across the fissure swarm in the northern part of the study area. It clearly defines a low-resistivity cap and an underlying high-resistivity core, but also other resistivity structures. The low-resistivity cap reaches an elevation of approximately 100 m a.s.l. in sounding 793957. The high-resistivity core is observed at an elevation of 250 m b.s.l. and is about 3 km wide. The high-resistivity core is indicated in three soundings (780960, 793957 and 800960) and is seen across the fissure swarm, and clearly defined in the cross-section. The low resistivity is very thick to the east but dips markedly to the west to an elevation of -900 m b.s.l.

Resistivity cross-section SW-NE (Figure 19) is very interesting because it lies along the fissure swarm and its length is about 12 km. In this cross-section, the low-resistivity cap reaches an elevation of
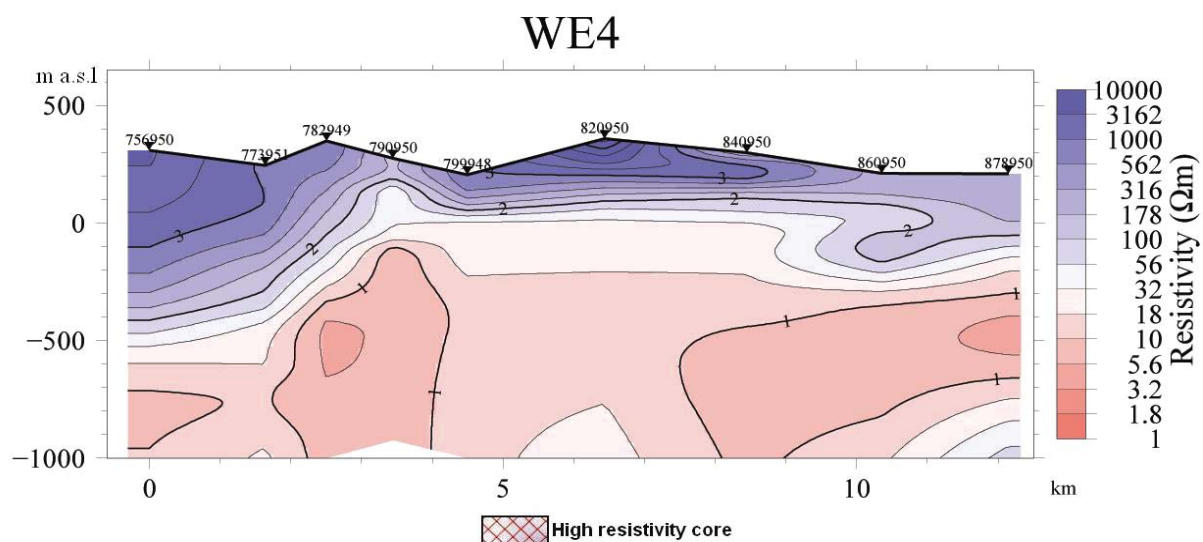
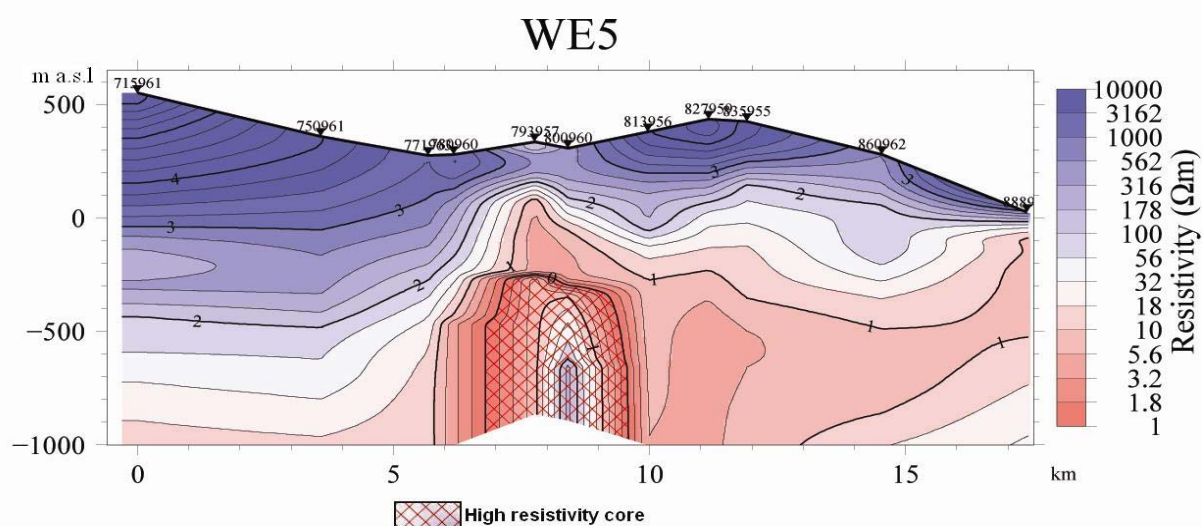FIGURE 17: TEM resistivity cross-section WE4
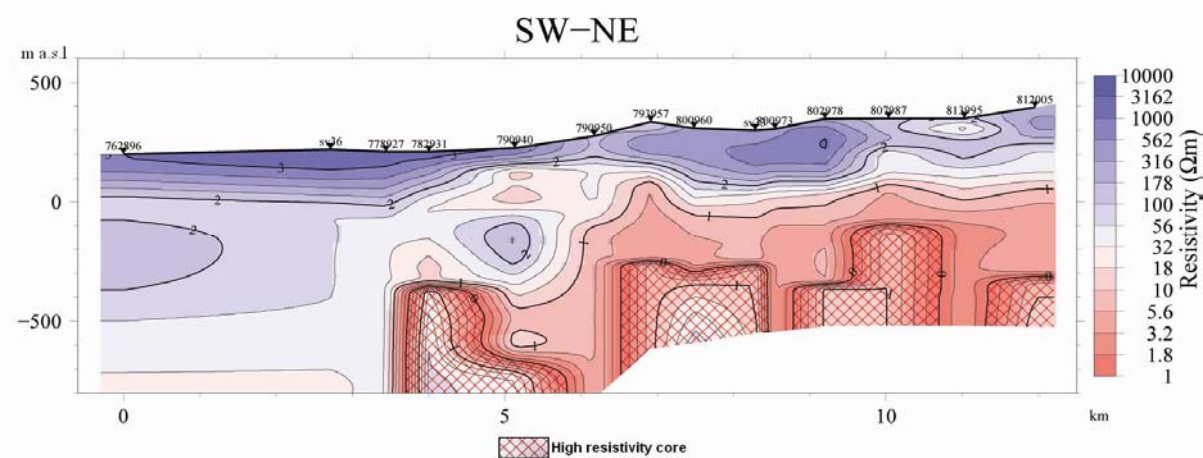

FIGURE 18: TEM resistivity cross-section WE5

FIGURE 19: TEM resistivity cross-section SW-NE

approximately 100 m a.s.l. and the high-resistivity core up to approximately 100 m b.s.l. The high-resistivity core is elongated along the fissure swarm, but is not continuous in this depth range. It looks as if the core is part of a SW-NE trending ridge with separate tops. Most likely these tops are connected at greater depth. The high-resistivity body is elevated in the northeast part of the fissure swarm and is connected with the Hengill central volcano.

7. CONCLUSIONS

This resistivity survey is a detailed survey in the southwest part of the Hengill central volcano. A total of 17 new TEM soundings were carried out in the study area and were combined to older interpreted soundings from previous TEM resistivity surveys conducted in the Hengill geothermal field. The data interpretation of the TEM survey was done using the 1D inversion program TEMTD. The interpreted data are presented in the form of resistivity cross-sections and iso-resistivity maps as well as data curves and layered models. The study area is at an elevation of approximately 300 m a.s.l.

The results of the TEM survey in the study area reveal the sequence of resistivity distribution of the rock formation in the uppermost kilometre. The resistivity in the uppermost 100-300 m is quite high, ranging between 100 and 6000 Ωm. This high-resistivity close to the surface, is correlated with fresh basalts and unaltered rocks. Thermal alteration is minimal in these rocks. Below that, the resistivity is low (the low resistivity cap), and it is obviously influenced by geothermal alteration, indicated by resistivities of 1-10 Ωm. The resistivity increases again at a deeper level by an order of magnitude, thus defining the high-resistivity core. The results of the TEM survey can be summarised in the following:

- A low-resistivity cap, underlain by a high-resistivity core, is present along the southwestern branch of the fissure swarm in the Hengill volcanic system.
- The high-resistivity core reaches an elevation of approximately 100 m b.s.l. which means that the top of the high-resistivity core is at 450-550 m depth from the surface of the study area.
- The temperature in the high-resistivity core is expected to exceed 230°C, provided there is equilibrium between the thermal alteration of the rock and the present temperature in the reservoir.
- The high-resistivity core is elongated along the fissure swarm.

The TEM resistivity survey, carried out in the southwest part of the Hengill area in 2006, indicates an extension of the Hengill geothermal field to the southwest along the NE-SW fissure swarm that intersects the Hengill central volcano.

REFERENCES

Anderson, D., 1979: The deep structure of continents. *J. of Geophys. Research, 84(B13),* 0148-0227.

Archie, G.E., 1942: The electrical resistivity log as an aid in determining some reservoir characteristics. *Tran. AIME, 146,* 54-67.

Árnason, K., 1989: *Central loop transient electromagnetic sounding over a horizontally layered earth.* Orkustofnun, Reykjavik, report OS-89032/JHD-06, 129 pp.

Árnason, K., 2006a: *Further exploration of the south part of the Hengill fissure swarm with resistivity soundings.* ISOR, Reykjavík, report ISOR-06118, 19 pp.

Árnason, K., 2006b: *TEMTD (Program for 1D inversion of central-loop TEM and MT data).* ISOR, Reykjavík, short manual 16 pp.

Árnason, K., Karlsdóttir, R., Eysteinsson, H., Flóvenz, Ó.G., and Gudlaugsson, S.Th., 2000: The resistivity structure of high-temperature geothermal systems in Iceland. *Proceedings of the World Geothermal Congress 2000, Kyushu-Tohoku, Japan,* 923-928.

Dakhnov, V.N., 1962: Geophysical well logging. *Q. Colorado Sch. Mines, 57-2*, 445 pp.

Fridleifsson, G.Ó, Ármannsson, H., Árnason, K., Bjarnason, I.Th., and Gíslason, G., 2003: Part I: Geosciences and site selection. In: Fridleifsson, G.Ó. (ed.), *Iceland Deep Drilling Project, feasibility report.* Orkustofnun, Reykjavik, report OS-2003-007, 104 pp.

Flóvenz, Ó.G., Georgsson, L.S., and Árnason, K., 1985: Resistivity structure of the upper crust in Iceland. *J. Geophys. Res., 90-B12,* 10,136-10,150.

Geonics Ltd, 1980: *Application of transient electromagnetic techniques.* Geonics Ltd., Technical note NT-17.

Georgsson, L.S., 1989: *Bakki and Litlaland in Ölfus. TEM-measurements in the summer 1989.* Orkustofnun, Reykjavík, report OS-89054/JHD-26 B (in Icelandic), 10 pp.

Hersir, G.P., and Björnsson, A., 1991: *Geophysical exploration for geothermal resources. Principles and applications.* UNU-GTP, Iceland, report 15, 94 pp.

ISL, 1999: *Liquid moulding.* ISL, Michigan State University, webpage islnotes.cps.msu.edu/trp/rtm/modl_mes.html .

Keary, P., and Brooks, M., 1992: *An introduction to geophysical exploration.* Blackwell Scientific Publications, Oxford, 254 pp.

Keller, G.V., and Frischknecht, F.C., 1966: *Electrical methods in geophysical prospecting.* Pergamon Press Ltd., Oxford, 527 pp.

Morris, F.H., and Becker A., 2001: *Berkeley course in applied geophysics.* University of California, Berkeley, Ca, unpublished lecture notes.

Quist, A.S., and Marshall, W.L., 1968: Electrical conductances of aqueous sodium chloride solutions from 0 to 800°C and at pressures to 4000 bars. *J. Phys. Chem., 72,* 684-703.

Rink, M. and Shopper, J.R. 1976: Pore structure and physical properties of porous sedimentary rocks. *Pure Appl. Geophys. 114,* 273-284.

Saemundsson, K., 1967: Vulkanismus und Tektonik des Hengill-Gebietes in Sudwest-Island (in German). *Acta Nat. Isl., II-7*, 195 pp.

Ward S.H. and Hohmann G.W., 1987: Electromagnetic theory for geophysical applications In: Nabighian, M.N. (ed.), *Electromagnetic methods in applied geophysics, volume I, theory.* Society of Exploration Geophysicists, Tulsa, OK, 131–311.

APPENDIX I: Plots of 1D Modelling of TEM sounding data

The measured TEM data curve is shown with red dots;   The calculated TEM data curve is in red; The 1D layered modelling is in green.